
Surface Catalytic Efficiency of Advanced Carbon Carbon Candidate Thermal Protection Materials for SSTO Vehicles

David A. Stewart, Ames Research Center, Moffett Field, California

February 1996



National Aeronautics and
Space Administration

Ames Research Center
Moffett Field, California 94035-1000

Surface Catalytic Efficiency of Advanced Carbon Carbon Candidate Thermal Protection Materials for SSTO Vehicles

DAVID A. STEWART

Ames Research Center

Summary

The catalytic efficiency (atom recombination coefficients) for advanced carbon carbon (ACC) thermal protection systems was calculated using arc-jet data. Both oxygen and nitrogen atom recombination coefficients were obtained for these systems up to temperatures of 1650 K. Optical and chemical stability of the candidate systems to the high energy hypersonic flow was also demonstrated during these tests.

Nomenclature

H_T	total enthalpy
h_D	enthalpy of formation
k_w	reaction rate constant
Le	Lewis number
M	molecular weight
M_f	Frozen Mach number
m_f	mass flow rate
P	pressure
Pr	Prandtl number
\dot{q}	heat flux
R	radius
s	arc length
Sc	Schmidt number
T	temperature
U	velocity
α	mass fraction
γ	recombination coefficient
ρ	density
μ	viscosity
\mathfrak{R}	gas constant

Subscripts

2	behind bow shock wave
A	air
e	boundary-layer edge
FF	flat-faced cylinder
i	chemical specie
N	nitrogen
O	oxygen
o	stagnation point
w	wall
∞	free stream

Introduction

Candidate ceramic thermal protection systems (TPS) for future space launch of single stage to orbit (SSTO) vehicles being considered as part of the Access-to-Space program includes metallic, fibrous insulation and coated carbon carbon (ref. 1). During hypersonic Earth entry, the high temperature air between the bow shock wave and the TPS surface will be partially dissociated into atoms. Therefore, the heat transferred to the surface will consist of chemical as well as sensible energy. The rate at which chemical energy is transferred (through nitrogen and oxygen atom recombination) to the material's surface is strongly influenced by its catalytic efficiency. This surface property must be included along with optical and thermal properties of the candidate system to accurately size the TPS for any proposed vehicle.

In this study, coefficients are reported for advanced carbon carbon (ACC) systems provided by NASA Langley Research Center and McDonnell Douglas Aerospace Corporation. These systems include the C-CAT ACC-4 (LTV and Carbon Advanced Technologies), LVP (Loral and Vought Process), and a vapor deposited silicon carbide system made by the Russians. The coefficients for three candidate carbon carbon systems were obtained using arc-jet data from tests conducted in the NASA

Ames Research Center Aerothermodynamic Heating Facility (AHF).

Arc-Jet Facility

A sketch of the facility and typical measuring equipment to obtain data for determining the surface catalytic efficiencies of selected TPS are shown in figure 1. The AHF uses a constricted arc heater to provide high-enthalpy dissociated hypersonic flow over a test model positioned downstream of a 16 deg conical nozzle (fig. 1(a)). Either nitrogen or air can be easily used as the test gas without altering the heater hardware. This permits quick, consecutive measurements of heat flux and temperature to be taken from a test model during its exposure to either test gas. Surface conditions on the test model are varied by changing either the exit diameter of the nozzle, the reservoir pressure, or the electrical power dissipated in the arc heater.

The geometric area ratio (nozzle exit to throat) of the facility can be varied from 64 to 400. Heater pressure can be varied from 0.68 atm to roughly 5.5 atm and the maximum power dissipation in the heater can be increased up to 20 MW. Stagnation point enthalpy was determined using a nozzle computer code, measurements of stagnation point pressure and heat flux to a hemisphere and Laser Induced Fluorescence (LIF) diagnostics (refs. 2 and 3).

A Pyrometer, radiometer, and copper hemisphere (with pressure orifice) were used to measure surface temperature, heat flux, and pressure during each test (fig. 1(b)).

Test Samples

Arc-Jet Tests

The samples were disks, roughly 0.060 cm thick and 7.11 cm in diameter, made from ACC and coated basically with glass and/or silicon carbide system. The C-CAT ACC-4 is an SiC conversion coating with a Type 1 sealant (sodium silicate-based glass over a coating of tetraethylortho-silicate (TEOS) glass). The LVP is a CVD SiC/SiB glass containing zirconium oxide. Finally, the Russian coating is a CVD SiC/HfB₂ system.

During the arc-jet tests, the samples were tested in a 15.2 cm diameter flat-faced cylinder (fig. 2). The front surface of the cylinder, made from using AETB-12 coated with TUF1. Each carbon carbon sample, cut in the shape of a 7.11 cm diameter disk, was mounted inside a retaining ring. A disk of AETB-12 insulation was placed behind the test sample. This assembly was used to hold the sample in the flat-faced cylinder. The retaining ring,

7.62 cm in diameter and 6.25 cm thick, was also made from AETB-12/TUF1. This arrangement resulted in the sample being recessed 0.3 cm below the front surface of the cylinder. However, earlier arc-jet tests showed that the recessed mounting of the sample did not affect the surface temperature or heat flux relative to a flush mounted sample (ref. 4). Finally, platinum/platinum/13% rhodium thermocouples were installed either just behind the sample or in the surface of the AETB insulation.

A reference model (flat-faced 5 deg cone) was used to aid in defining the test condition during each exposure. It was made using AETB-12 rigid fibrous insulation. The front surface of the cone was coated with a reaction cured glass (RCG). The RCG coating (a full dense borosilicate glass) was applied as a surface coating and was approximately 0.030 cm thick. The cone had a base diameter of 8.89 cm, corner radius of 1.3 cm, and a thickness of 6.35 cm. A threaded aluminum mounting ring was bonded into the base of each cone so that they could be attached to a water-cooled support. Surface thermocouples (platinum/platinum/13% rhodium) were installed at the stagnation point of each cone.

The test configurations were designed to ensure an adiabatic back wall and uniform temperature and pressure distributions across the front surface of the test samples.

Analysis

To obtain coefficients for candidate TPS from room temperature to their upper use temperature requires data from both a side-arm-reactor and arc-jet facilities (ref. 5) In this study, samples were only available for testing in the arc-jet; therefore, this section outlines the basic approach used in calculating the atom recombination coefficients from measured data taken in this facility.

Atom recombination coefficients for the ACC systems were calculated using the "Stewart-Chen" SCFC code (ref. 2). This code calculates the surface coefficients assuming frozen chemistry and incorporates Goulard's theory as part of a nozzle program written by Yoshikawa and Katzen (refs. 6 and 7).

Goulard's theory:

$$\begin{aligned} \dot{q}_w = & 0.66 \text{Pr}^{-2/3} (\rho_2 \mu_2)^{1/2} \\ & \times \left[\left(\frac{du_e}{ds} \right) \text{FF} \right]^{1/2} [H_{e0} - H_w] \\ & \times \left[1 + (\text{Le}^{2/3} \phi_O - 1) \alpha_O h_D / (H_{e0} - H_w) \right. \\ & \left. + (\text{Le}^{2/3} \phi_N - 1) \alpha_N h_D / (H_{e0} - H_w) \right] \end{aligned} \quad (1)$$

where

$$\phi_i = \left\{ 1 + 0.47 Sc^{-2/3} [2(du_e / ds)_{FF} \times \rho_2 \mu_2] / p_w k_{wi} \right\}$$

To calculate the reaction rate constant from Goulard's theory (ref. 6) requires inputs of gas properties from the free-stream, shock-layer and stagnation-point regions of the flow. Gas properties in the code are obtained from the Aerotherm Chemical Equilibrium (ACE) code (ref. 8) and using Gupta's thermodynamic properties (ref. 9).

The state-of-the-gas in the free-stream was defined with the frozen Mach number and was determined by iteration process between the total enthalpy, velocity or nitrogen mass fraction that were obtained from the LIF measurements. The frozen Mach number varied from 1.2 to 2.5 for the test conditions used in this study. Corresponding free-stream velocity, relative nitrogen atom concentrations, and gas temperatures for these arc-jet tests are shown in figures 3–6. Properties behind the bow shock wave were calculated assuming a weak bow shock wave in front of the blunt models (based on the Knudsen number). In addition, the solution requires the velocity gradient at the stagnation point of the model. The velocity gradient was derived from measured heat fluxes taken from both a hemisphere and flat-faced cylinder (fig. 7).

Finally, using the two basic assumptions: (1) a first-order reaction occurs on the surface of the coating, and (2) the energy accommodation coefficient (β) for the material is unity. The following well-known expression can be used to calculate the atom recombination coefficients for the material.

$$\gamma_i = k_{wi} / \sqrt{R T_w / 2\pi M_i} \quad (2)$$

Relative Coefficient for Air

The SCFC code also calculates a relative reaction rate constant (k_w) for each material using only air test data. The equation, developed by Rosner (ref. 10), assumes a partially dissociated diatomic gas, frozen flow (gas phase recombination in the shock layer is neglected) and finally $T_w \ll T_{e0}$ so that $\alpha_{ieq}(T_w, p) \ll \alpha_{ie}$. With these assumptions he showed that the following semi-empirical relationship results:

$$k_w = (\rho_\infty U_\infty St) / \rho_w \cdot Le^{2/3} \times (q_0 - q_{min}) / (q_{max} - q_0) \quad (3)$$

Parameters (q_{min}) and (q_{max}) were obtained from Goulard's theory by setting $\phi = 0$ and $\phi = 1.0$ respectively. The stagnation point heat flux (q_0), used in equation 1, is equal to the radiated heat flux plus the amount conducted into the model. The relative recombination

coefficient (γ_A) for the TPS is calculated again using equation 2.

Experiments

Arc Jet

A summary of the arc-jet tests is given in table 1. The sample number, material identification, total exposure, surface temperature, and environments are listed. Mass loss measurements were taken from samples LVP (d-2) and C-CAT (d3-3) during a total of 200 min of exposure to the hypersonic arc-jet air stream. Data were taken after each 10 min exposure to the arc-jet stream. Samples used to obtain data for calculating the recombination coefficients were tested in either nitrogen or air streams for 180 sec. These samples were tested from one to five times over a range of surface temperatures from roughly 1200 K to 1730 K. Surface pressures ranged from 0.005 atm to 0.035 atm and total enthalpies from 12.8 MJ/kg to 25 MJ/kg.

During each test, the heat flux to an RCG coated model was measured along with the heat flux to the test model using a radiometer. Surface temperature data were obtained from both models using thermocouple and pyrometer measurements. During each test, stagnation point pressure and heat flux to a water-cooled copper 10.16 cm diameter hemisphere were measured, and free-stream properties were determined from data taken using LIF measurement techniques (refs. 2 and 3). In addition to calculating atom recombination coefficients for each sample, surface characterization data were also obtained during the study. First, pre and post-test room temperature spectral reflectance measurements were made using a BIO-RAD model FTS 40 (wavelength range 0.25 micron to 2.5 microns) and a Perkin Elmer model 310 (wavelength range 2.5 microns to 20 microns) spectrophotometer. Second, mass loss data were obtained from a C-CAT and LVP sample after each 10 min exposure in air (these samples were tested for a total of 200 min). Finally, pre and post-test elemental chemical analysis of each sample was made using X-ray fluorescence measurements.

Results and Discussion

Initial arc-jet exposure of C-CAT and LVP samples resulted in a weight loss of 0.1 percent and 0.4 percent loss respectively (fig. 8). Upon further exposure of both samples to the arc-jet a continuous weight gain occurred. Surface chemistry data show the loss of sodium and carbon from the C-CAT sample, and of zirconium and oxygen from the LVP sample after arc-jet exposure

(figs. 9–11). Also, these data show that the Russian sample remained relatively chemically stable during arc-jet exposure. The effect of the arc-jet on surface chemistry of the samples is apparent from the photographs of the C-CAT and LVP samples after arc-jet exposures of 150 min (figs. 12 and 13). The photographs show that the surfaces of these samples have become lighter in color. Effect of surface chemistry on total hemispherical emittance is demonstrated using values calculated from room temperature spectral reflectance data. The calculation using the reflectance data assumed that the surface of the samples was nontransparent. These values are plotted as a function of surface temperature in figure 14. The predicted total hemispherical emittance compared well with values obtained from arc-jet data. The data suggest that the change in emittance for the C-CAT and LVP systems occurred during their initial exposures. The change in emittance for the Russian sample occurred gradually over several tests. Finally, the atom recombination coefficients for the three ACC systems were calculated using the arc-jet data and the SCFC code (figs. 15–18). Arrhenius expressions fitted to the calculated coefficients for the three ACC samples are given below:

C-CAT:

(Nitrogen)

$$(1200 \leq T_w \leq 1538 \text{ K}) \quad \gamma_N = 10 e^{-10360/T_w} \quad \text{(C-CAT-1)}$$

$$(T_w \geq 1538 \text{ K}) \quad \gamma_N = 6.2 \times 10^{-6} e^{12100/T_w} \quad \text{(C-CAT-2)}$$

(Oxygen)

$$(1200 \leq T_w \leq 1368 \text{ K}) \quad \gamma_O = 13.5 e^{-8350/T_w} \quad \text{(C-CAT-3)}$$

$$(T_w \geq 1368 \text{ K}) \quad \gamma_O = 5.0 \times 10^{-8} e^{18023/T_w} \quad \text{(C-CAT-4)}$$

(Air)

$$(1200 \leq T_w \leq 1470 \text{ K}) \quad \gamma_A = 6.5 e^{-4410/T_w} \quad \text{(C-CAT-5)}$$

$$(T_w \geq 1470 \text{ K}) \quad \gamma_A = 2.0 \times 10^{-7} e^{17750/T_w} \quad \text{(C-CAT-6)}$$

LVP:

(Nitrogen)

$$(1200 \leq T_w \leq 1538 \text{ K}) \quad \gamma_N = 0.06 e^{-2605/T_w} \quad \text{(LVP-1)}$$

$$(T_w \geq 1538 \text{ K}) \quad \gamma_N = 1.5 \times 10^{-5} e^{10080/T_w} \quad \text{(LVP-2)}$$

(Oxygen)

$$(1200 \leq T_w < 1500 \text{ K}) \quad \gamma_O = 7.5 e^{-8283/T_w} \quad \text{(LVP-3)}$$

$$(T_w \geq 1500 \text{ K}) \quad \gamma_O = 2.5 \times 10^{-7} e^{17533/T_w} \quad \text{(LVP-4)}$$

(Air)

$$(1200 \leq T_w < 1538 \text{ K}) \quad \gamma_A = 0.08 e^{-2518/T_w} \quad \text{(LVP-5)}$$

$$(T_w > 1538 \text{ K}) \quad \gamma_A = 0.003 e^{2653/T_w} \quad \text{(LVP-6)}$$

Russian ACC:

(Nitrogen)

$$(T_w \geq 1250 \text{ K}) \quad \gamma_N = 0.0737 e^{-2361/T_w} \quad \text{(Russ-1)}$$

(Oxygen)

$$(T_w \geq 1250 \text{ K}) \quad \gamma_O = 4.2 \times 10^{-8} e^{17533/T_w} \quad \text{(Russ-2)}$$

(Air)

$$(T_w \geq 1250 \text{ K}) \quad \gamma_A = 8.0 \times 10^{-4} e^{5040/T_w} \quad \text{(Russ-3)}$$

In general, the figures show that the coefficients are unique surface properties of each TPS. Note that the coefficients for the C-CAT and LVP systems have similar profiles for both nitrogen and oxygen atoms. C-CAT and LVP, which were covered with basically a glass or oxide,

have similar characteristics to RCG (a reaction cured glass that is being used on the Shuttle Orbiter) (fig. 19). The decrease in the oxygen atom recombination coefficient for the C-CAT coating at a lower temperature than for the LVP system suggests that the glass coating on this sample has a lower viscosity than RCG. The coefficients for the Russian system are typical for a silicon carbide surface (see ref. 5). The coefficient for atomic nitrogen increased with increased temperature whereas the coefficient for atomic oxygen decreased. The expressions for the Russian sample are similar to TABI (a silicon carbide blanket), in that the atomic nitrogen is more susceptible to recombining at the surface of the TPS than atomic oxygen. To fully define the coefficients for all three systems, additional data from the side-arm-reactor or flow reactor are needed in order to calculate values at lower temperatures.

Conclusions

Atom recombination coefficients and surface characterization data for three ACC system candidates were obtained during arc-jet exposures. These data were obtained from these systems over surface temperatures ranging from roughly 1200 K to 1800 K. Results from this study showed:

1. Total hemispherical emittance of C-CAT and LVP samples decreased after short arc-jet exposure in air.
2. Total hemispherical emittance of the Russian sample increased during arc-jet exposure in air.
3. Both the C-CAT and LVP ACC systems were relatively stable and showed weight gain after an initial weight loss during their first arc-jet exposure.
4. Both C-CAT and LVP samples did show mass loss during the initial arc-jet exposure of these samples due to volatilization of unstable species (sodium, etc.).
5. Atom recombination coefficients are unique surface properties for each TPS.
6. More extensive data from the side-arm reactor are needed on the ACC system to fully define their surface catalytic efficiency and improve the accurate predictions of the heating over an SSTO.

References

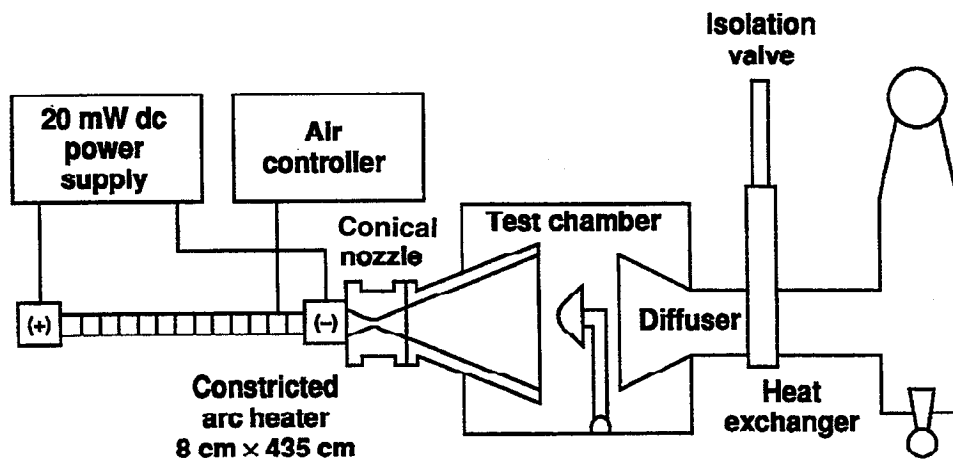
1. Office of Space Systems Development, NASA Headquarters: Access to Space Study. Summary Report, January 1994. AIAA J., vol. 2, May 1965, pp. 945-948.
2. Stewart, D. A.; Chen, Y. K.; Bamford, D. J.; and Romanovsky, A. B.: Predicting Material Surface Catalytic Efficiency using Arc-jet Tests. AIAA Paper 95-2013, June 1995.
3. Bamford, J. B.; O'Keefe, A.; Babikian, D. S.; Stewart, D. A.; and Strawa, A. W.: Characterization of Arc-Jet Flows Using Laser-Induced Fluorescence. AIAA Paper 94-0690, Jan. 1994.
4. Stewart, D. A.; Henline, W. D.; Kolodziej, P.; and Pincha, E. M. W.: Effect of Surface Catalysis on Heating to Ceramic Coated Thermal Protection Systems for Transatmospheric Vehicles. AIAA Paper 88-2706, June 1988.
5. Stewart, D. A.; Pallix, J.; and Esfahani, L.: Surface Catalytic Efficiency of Candidate Ceramic Thermal Protection Materials for SSTO. CDTM-20007, Mar. 1995.
6. Goulard, R.: On Catalytic Recombination Rates in Hypersonic Stagnation Heat Transfer. *Jet Propulsion*, vol. 28, no. 11, Nov. 1958, pp. 737-745.
7. Yoshikawa, K. K.; and Katzen, E. D.: Charts for Air-Flow Properties in Equilibrium and Frozen Flows in Hypervelocity Nozzles. NASA TN D-693, 1961.
8. Tong, H: Non-equilibrium Chemistry Boundary Layer Integral Matrix Procedure. Acurex Corp., Mountain View, Calif., Aerotherm Dept., UM-73, Apr. 1973.
9. Gupta, R. N.; Thompson, R. A.; and Kam-Pui, L.: A Review of Reaction Rates and Thermodynamic and Transport Properties for an 11 Species Air Model for Chemical and Thermal Non equilibrium Calculations to 30,000 K. NASA RP-1232, Aug. 1990.
10. Rosner, D. E.: Analysis of Air Arc-Tunnel Data. AIAA J., vol. 2, May 1965, pp. 945-948.

Table 1. Summary of ACC arc-jet tests

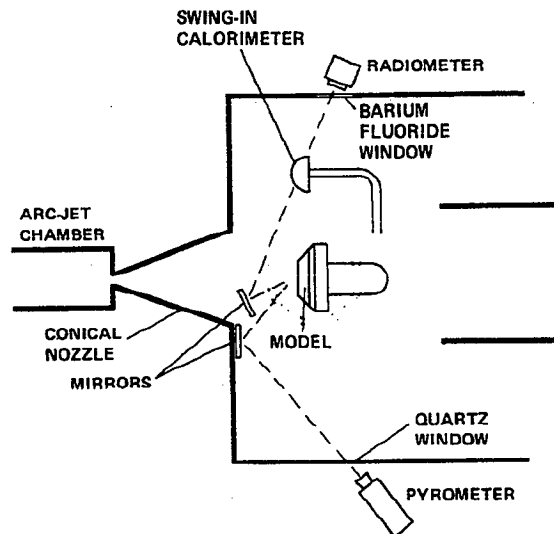
Sample No.	Material	Total exposure, min.	Range Tw, K	Range Heo, MJ/kg	Gas
LVP d-1	2328-58B	15	1207–1624	16.3–21.2	Nitrogen
d-2	2328-58C	200 ^a	1367	18.6	Air
d-3	2328-58D	15	1187–1680	14.5–19.8	Air
d-4	2328-58E	Pre-test	–	–	–
CCAT d3-1	ACC-4 System 3	15	1222–1724	15.6–21.4	Nitrogen
d3-2	ACC-4 System 3	15	1231–1667	15.1–18.6	Air
d3-2	ACC-4 System 3	3	1710	20.6	Nitrogen
d3-3	ACC-4 System 3	200 ^a	1367	15.6	Air
d3-4	ACC-4 System 3	Pre-test	–	–	–
ACC-R Partial	Russian	Pre-test	–	–	–
ACC-R	Russian	15	1279–1507	17.4–20.9	Air
ACC-R	Russian	12	1219–1606	16.2–21.9	Nitrogen

Surface catalysis, 3 min each exposure.

^aMass loss, 10 min each exposure.

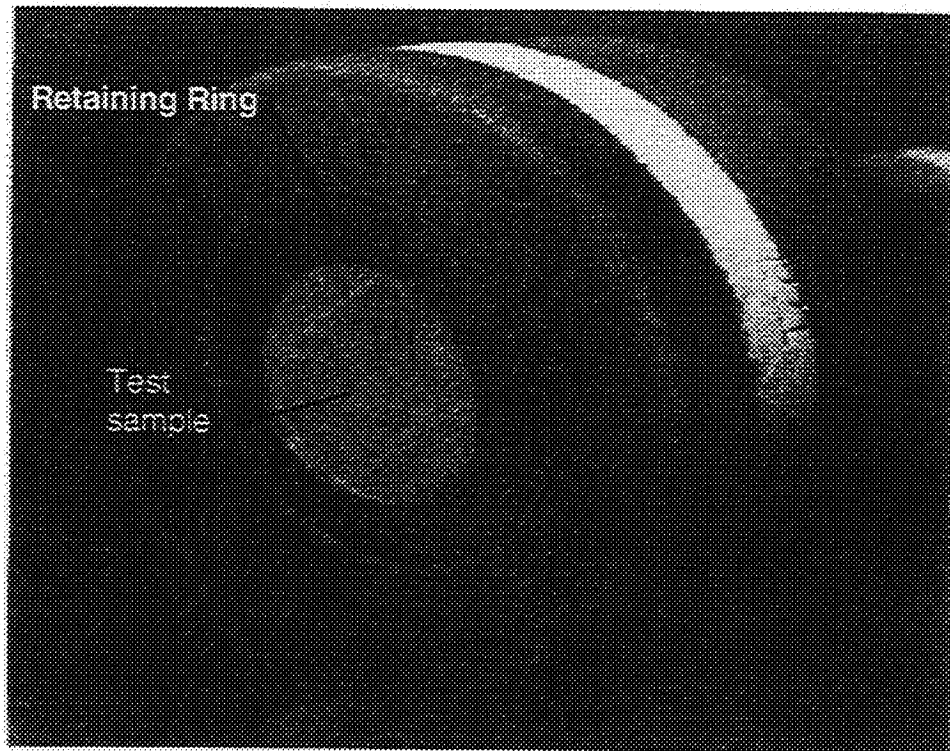


(a) Aerothermodynamic Heating Facility

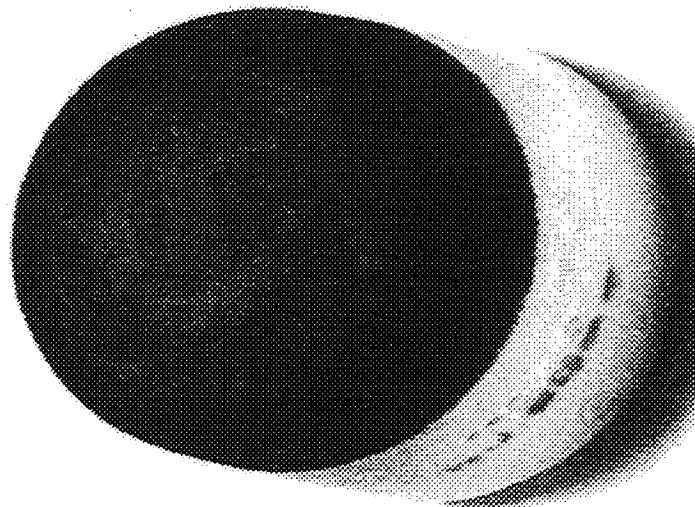


(b) Test arrangement

Figure 1. Arc-Jet Facility.



(a) Cylindrical sample holder



(b) Conical sample

Figure 2. Test models.

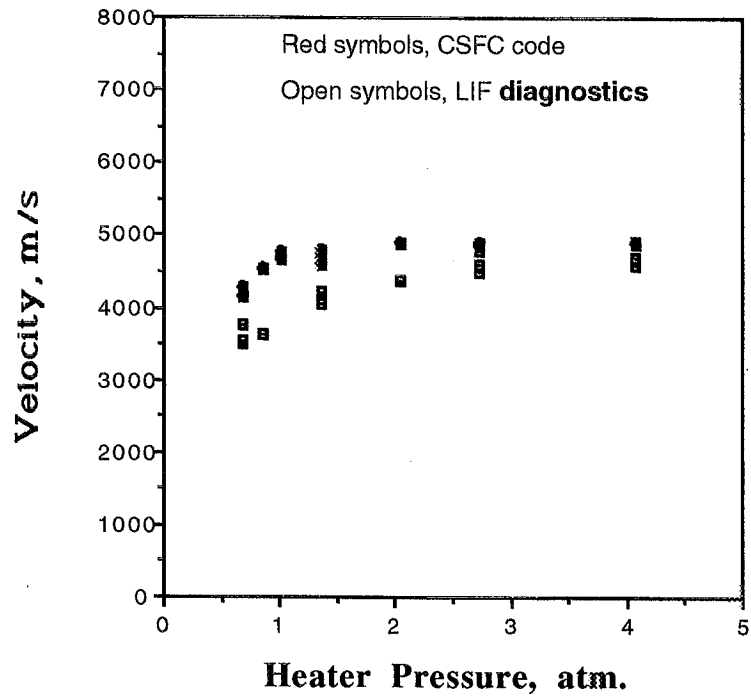


Figure 3. Correlation of predicted velocity in air from SCFC code and laser diagnostics.

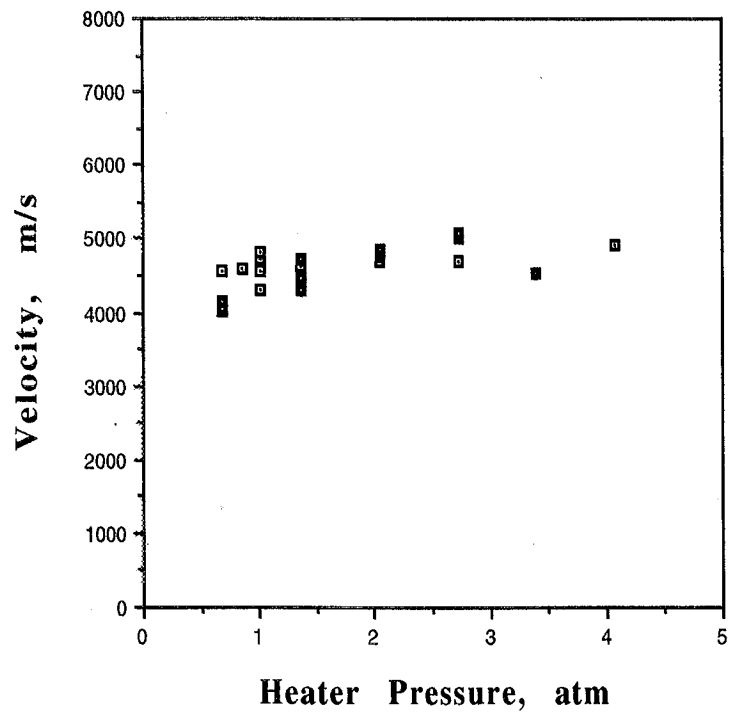


Figure 4. Comparison between predicted and calculated velocities in nitrogen streams.

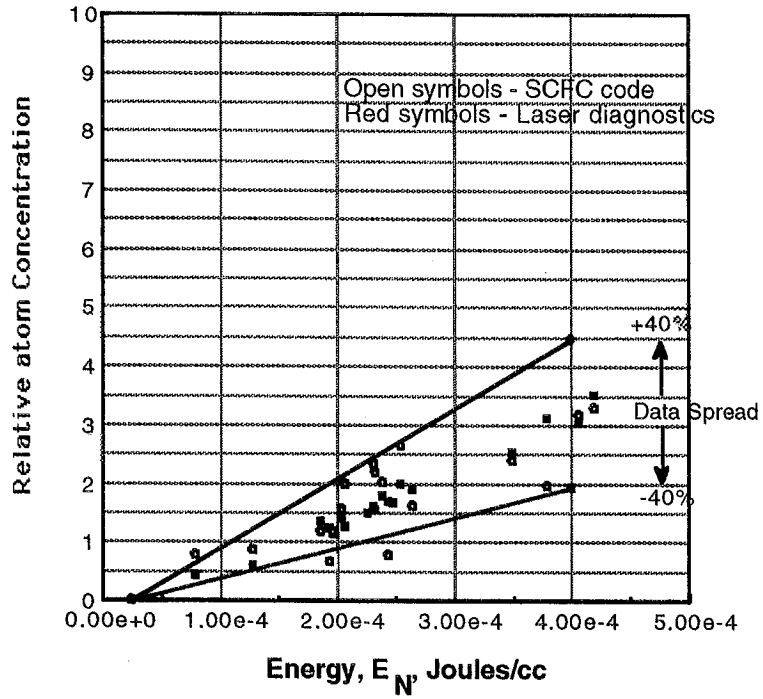


Figure 5. Predicted atomic nitrogen concentration in hypersonic air stream.

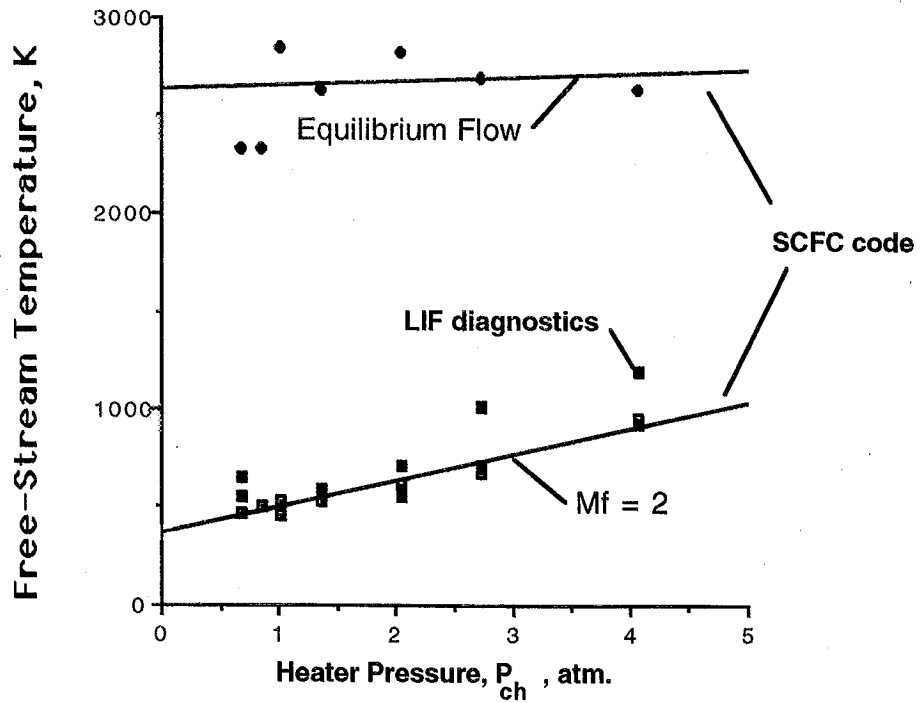


Figure 6. Predicted free-stream temperature in hypersonic air stream.

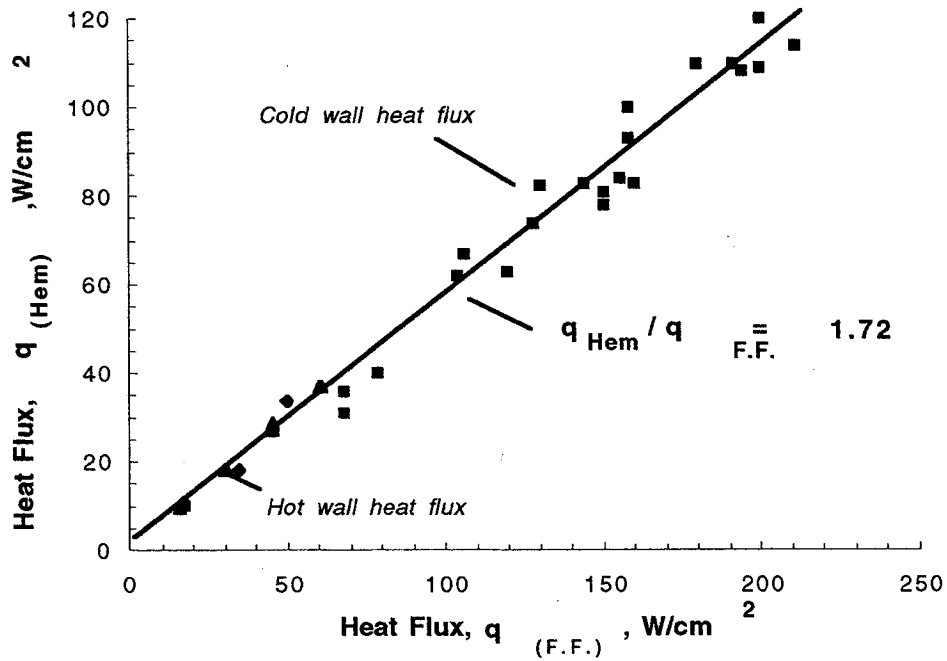


Figure 7. Correlation of stagnation point heat flux between hemisphere and flat-faced cylinder.

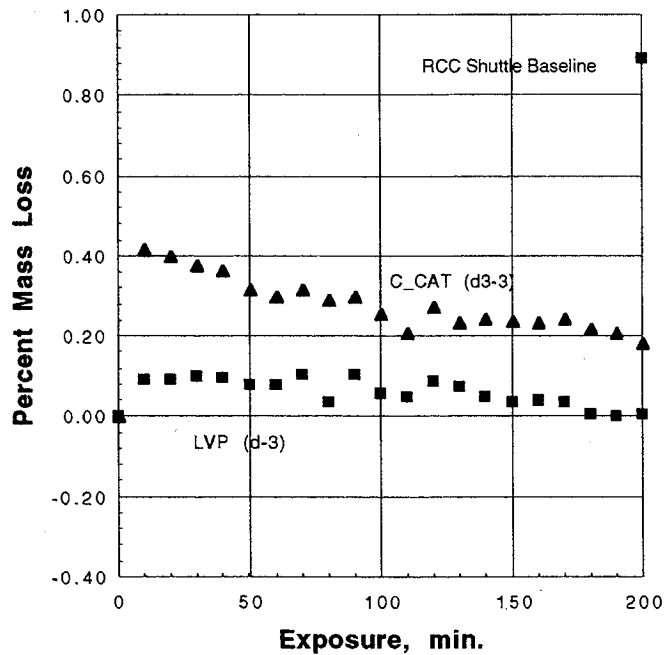
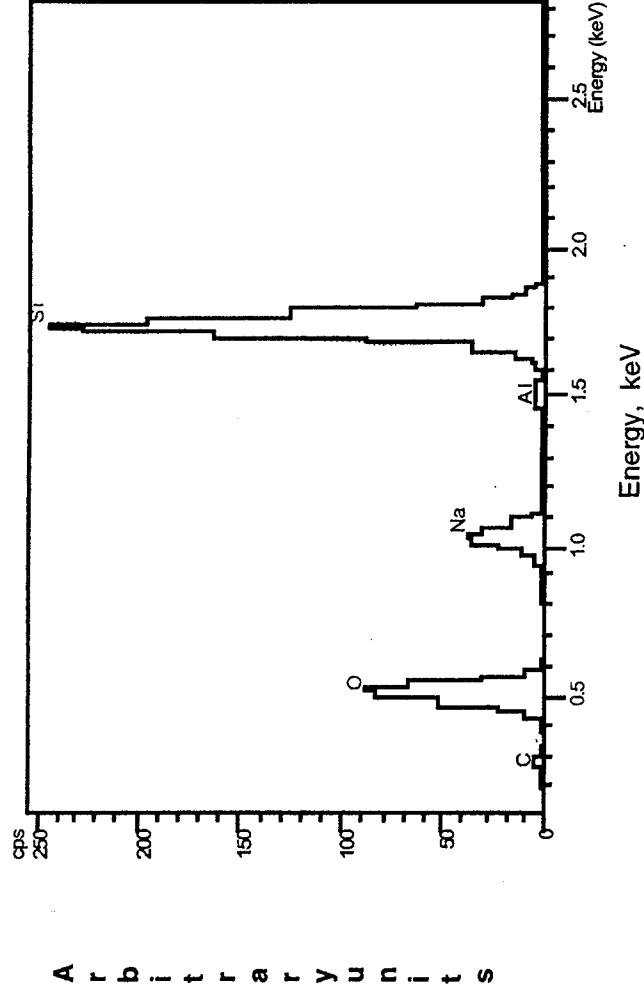
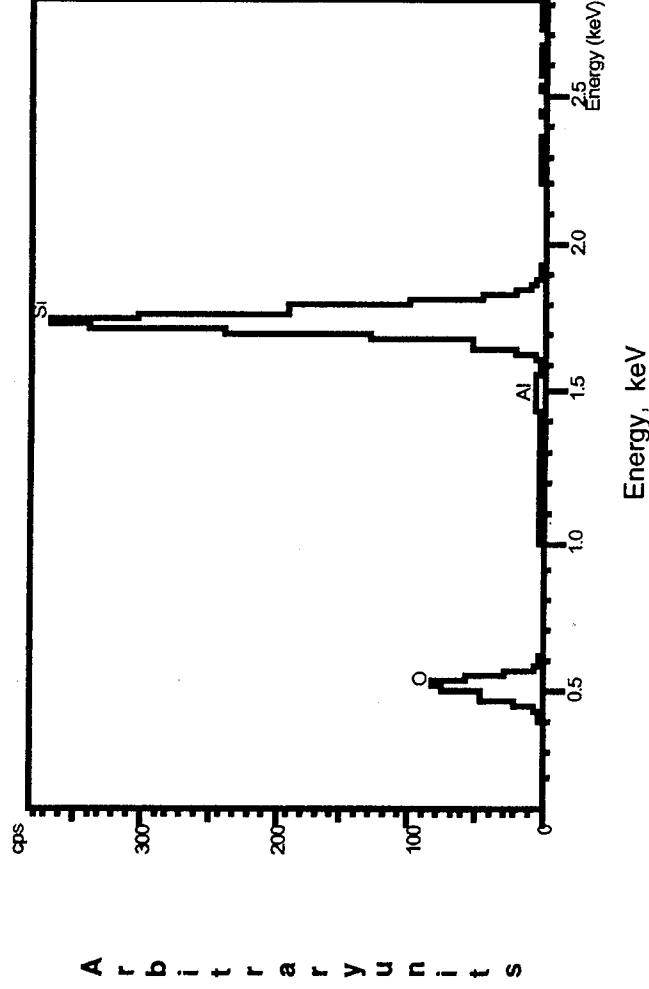


Figure 8. Measured mass loss from C-CAT and LVP samples after arc-jet exposure in air.

T_w = 1367 K, P_w = 0.01 atm. Heo = 19.8 MJ/kg

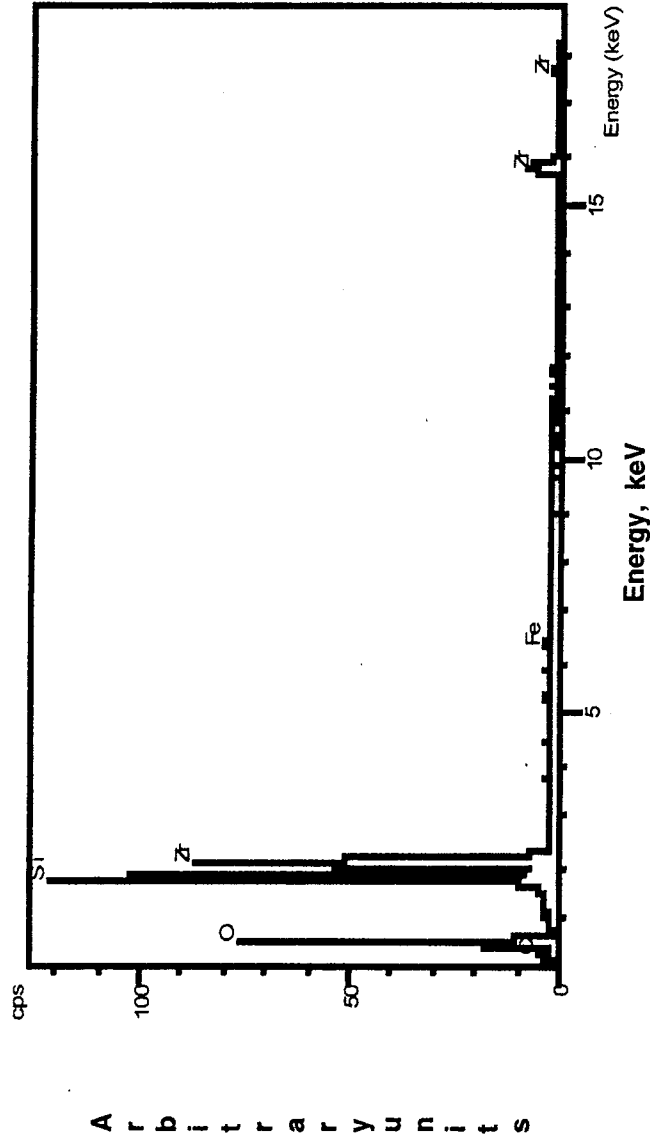


(a) Pre test

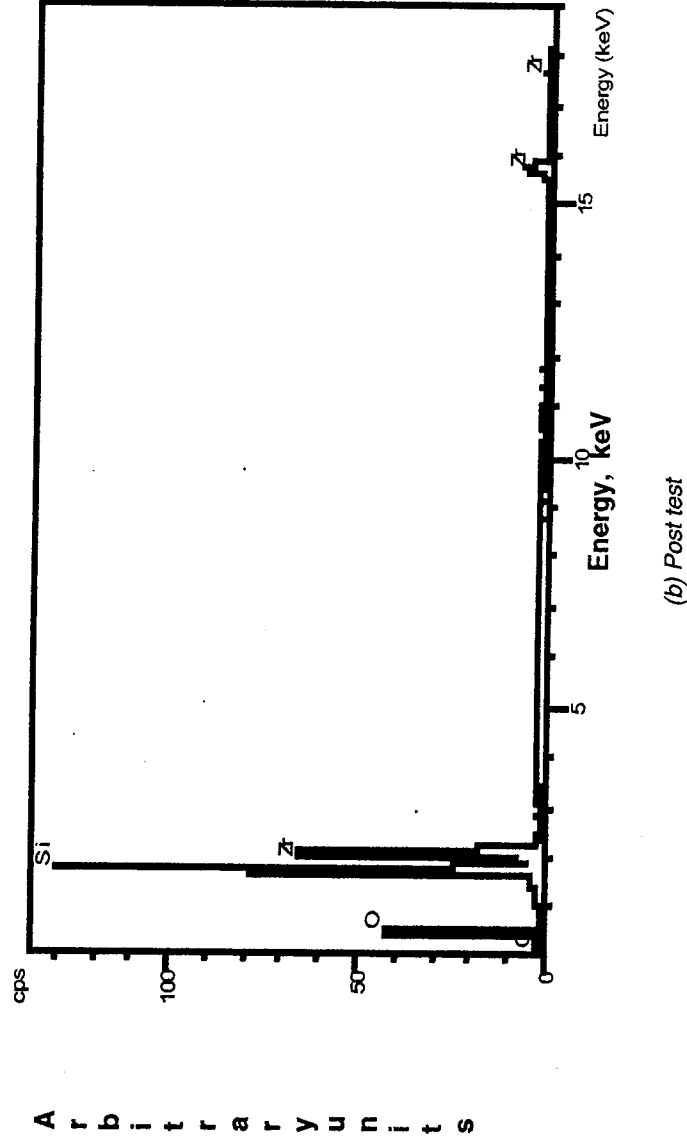


(b) Post test

Figure 9. Surface composition of C-CAT sample before and after arc-jet exposure.

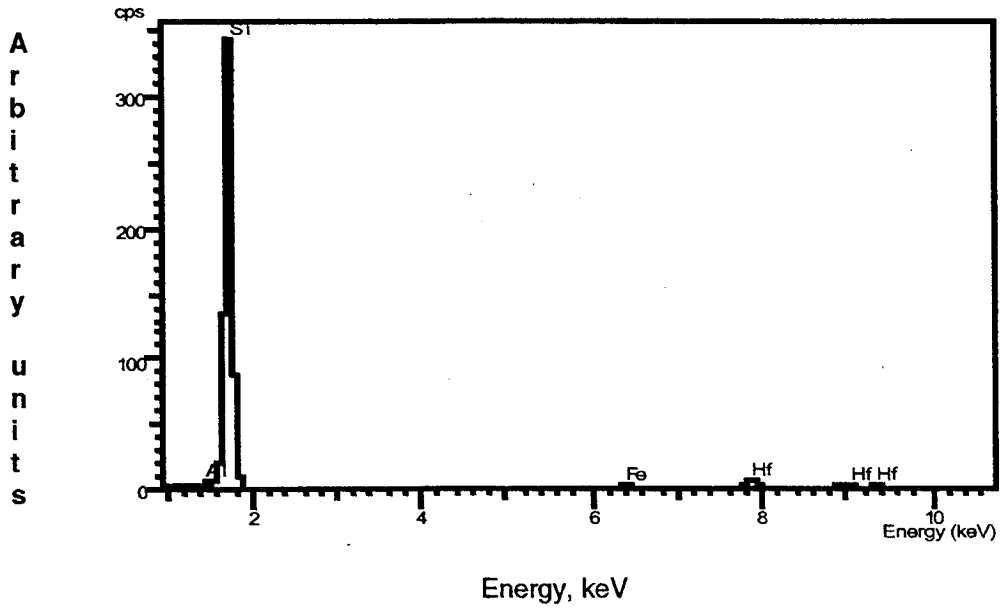


(a) Pre test

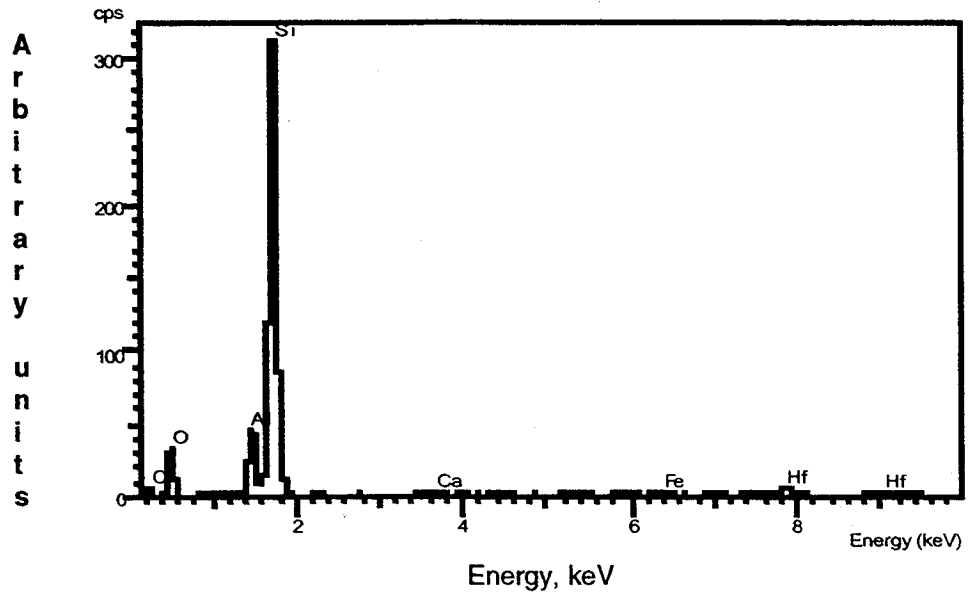


(b) Post test

Figure 10. Surface composition of LVP sample before and after arc-jet exposure.

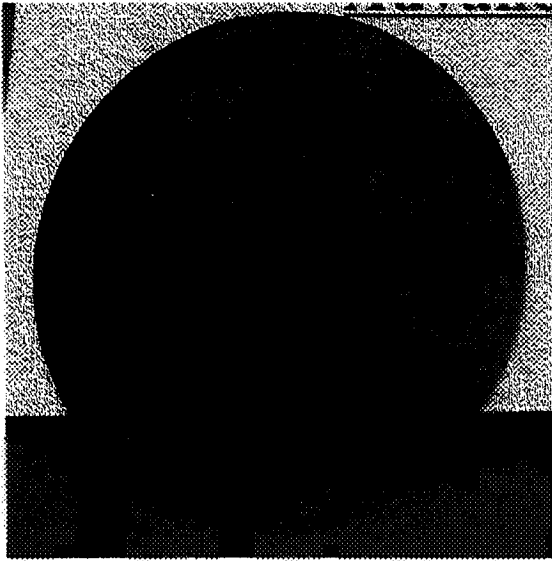


(a) Pre test



(b) Post test

Figure 11. Surface composition of the Russian ACC sample before and after arc-jet exposure.

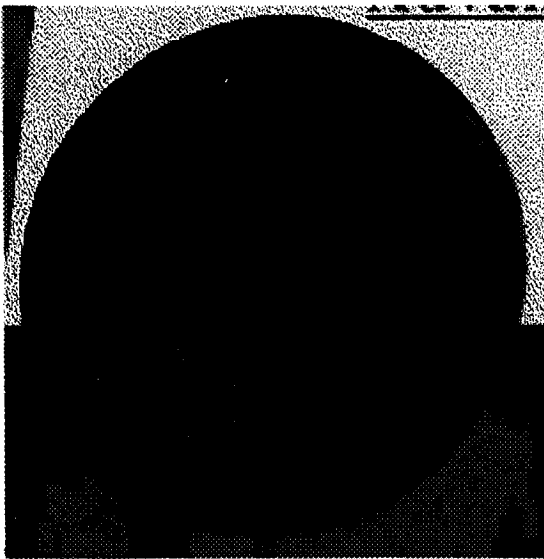


(a) Pre test

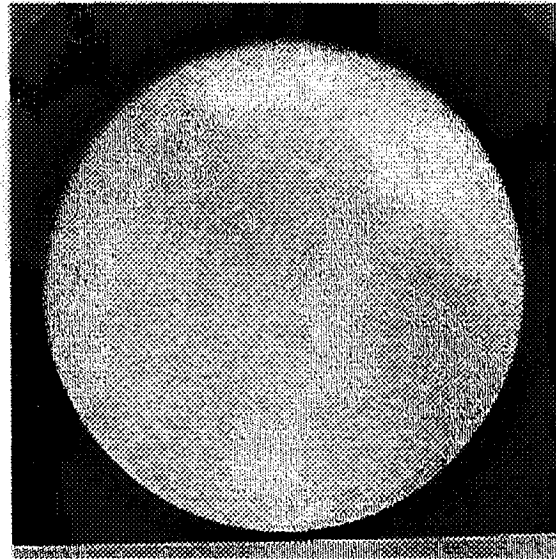


(b) Post test

Figure 12. Photographs of C-CAT sample before and after 150 min of arc-jet exposure.



(a) Pre test

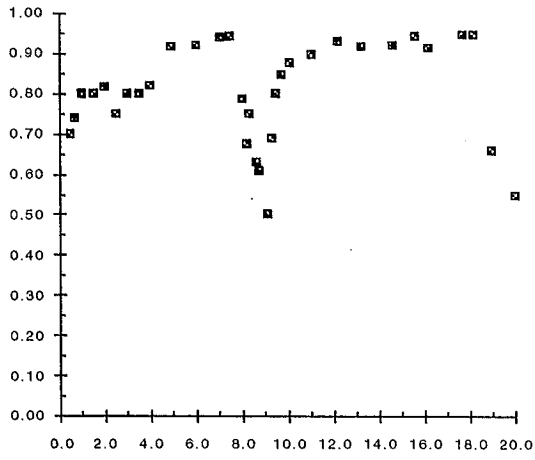


(b) Post test

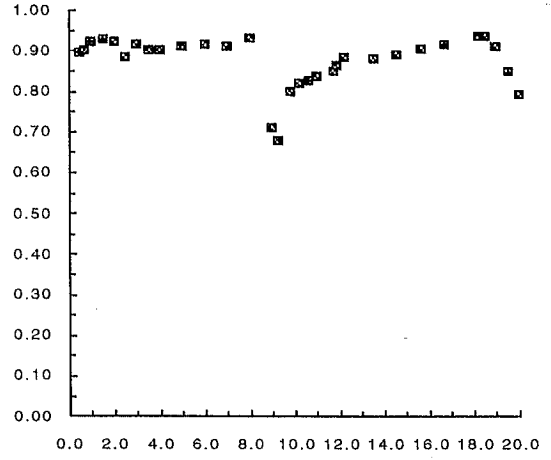
Figure 13. Photographs of LVP sample before and after 150 min of arc-jet exposure.

S
p
e
c
t
r
a
l

Pre Test

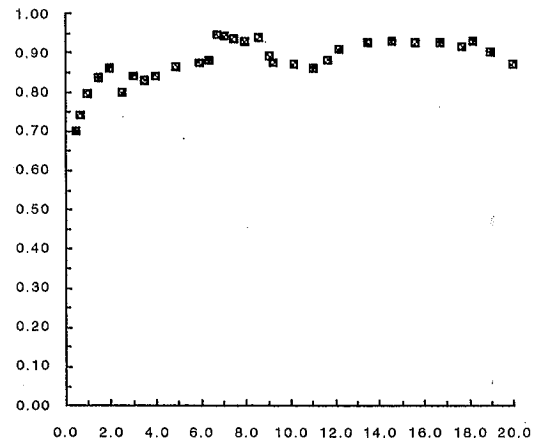
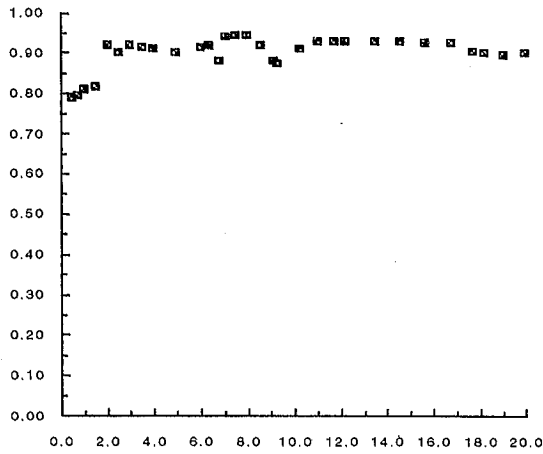


Post Test



(a) C-CAT

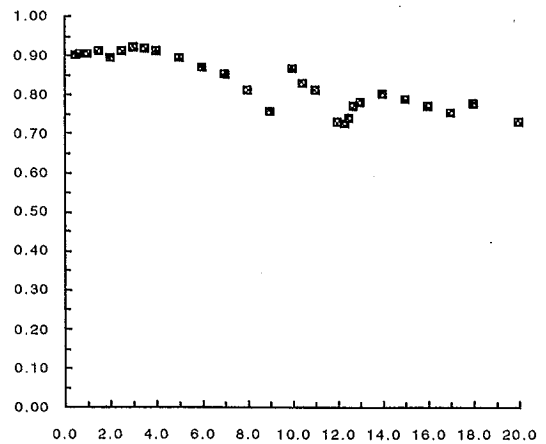
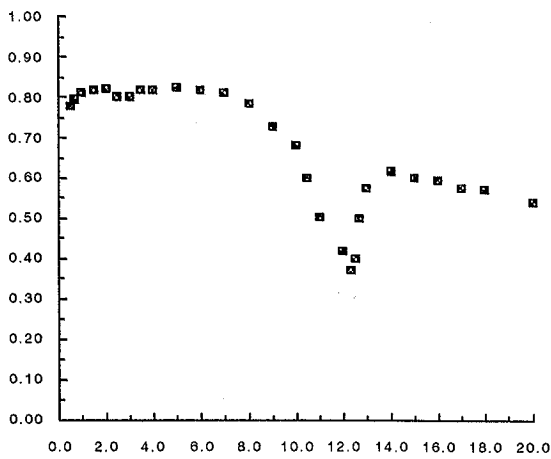
H
e
m
i
s
p
h
e
r
i
c
a
l



(b) LVP

E
m
i
t
t
a
n
c
e

 ϵ_λ



Wavelength, λ, microns

Wavelength, λ, microns

(c) Russian

Figure 14. Effect of arc-jet exposure on optical properties of ACC.

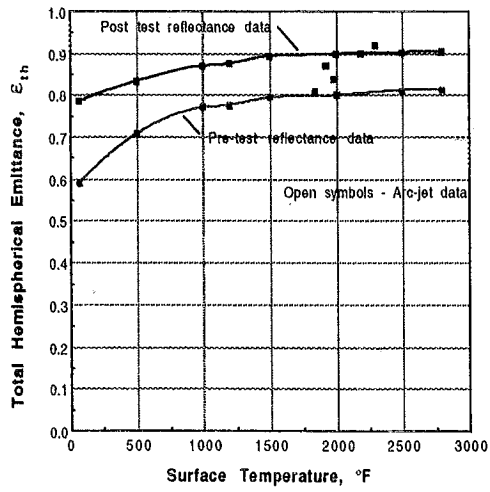
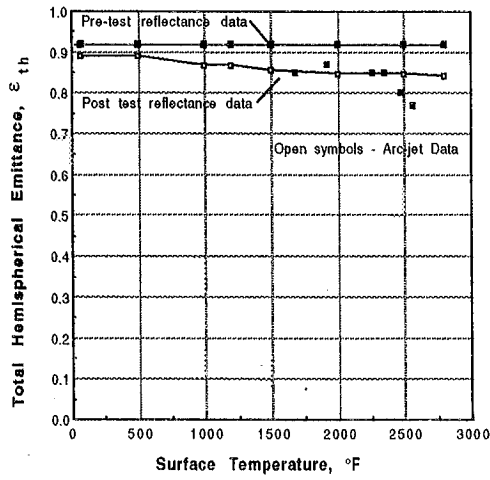
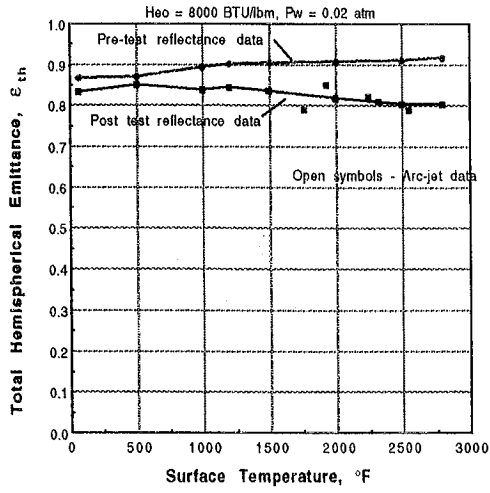
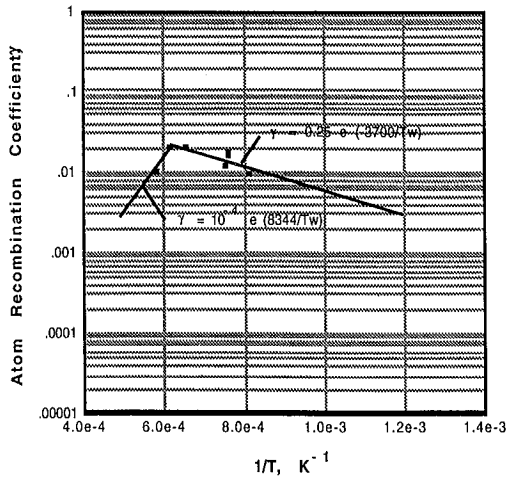
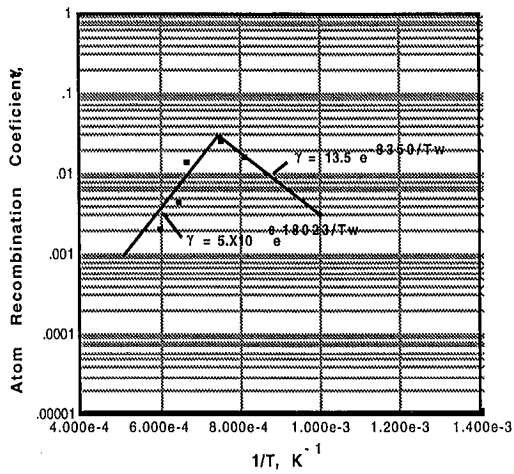


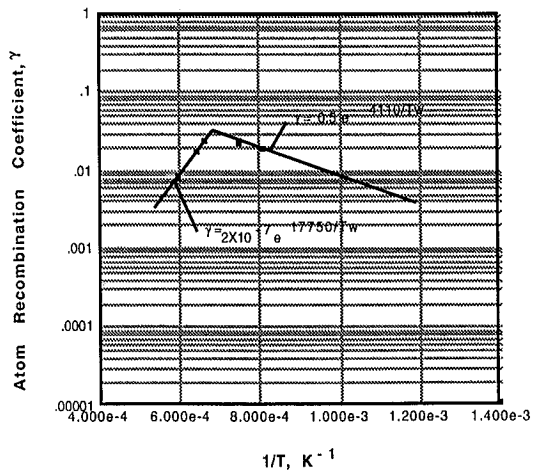
Figure 15. Total hemispherical emittance.



(a) Nitrogen

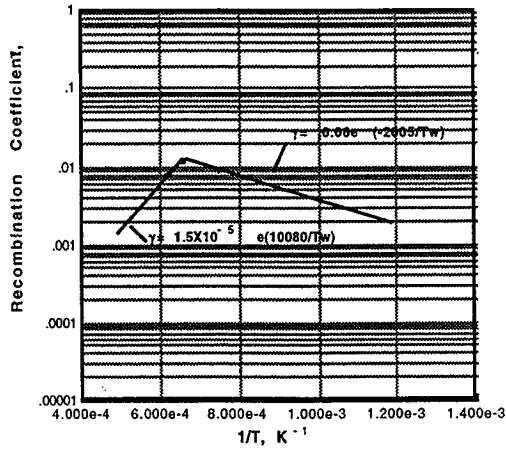


(b) Oxygen

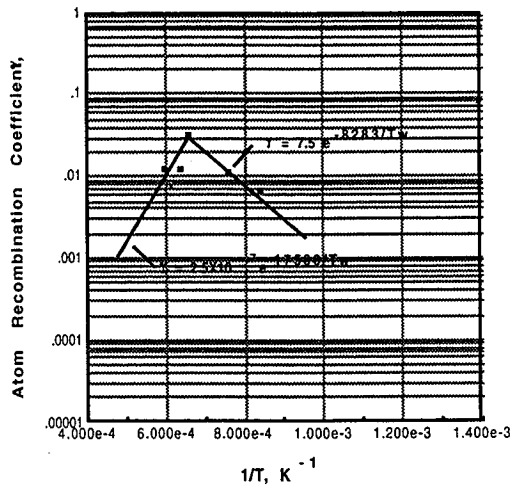


(c) Air

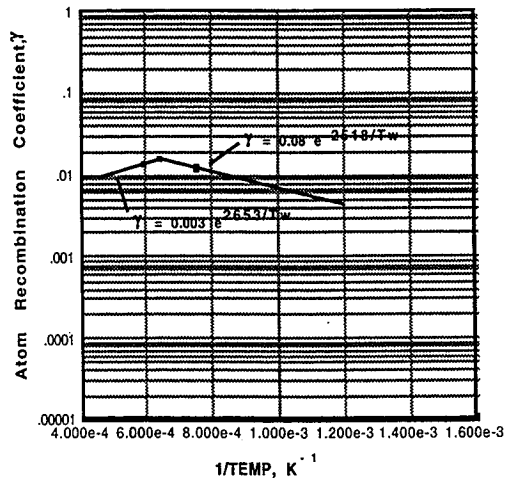
Figure 16. Atom recombination coefficients for C-CAT.



(a) Nitrogen



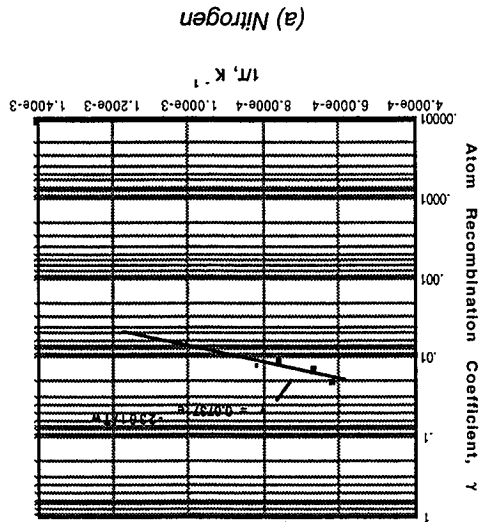
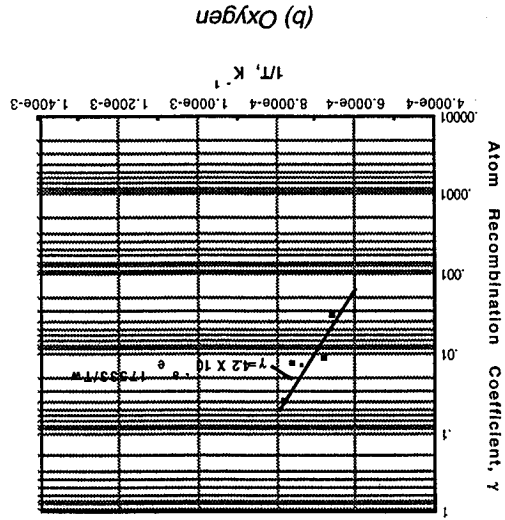
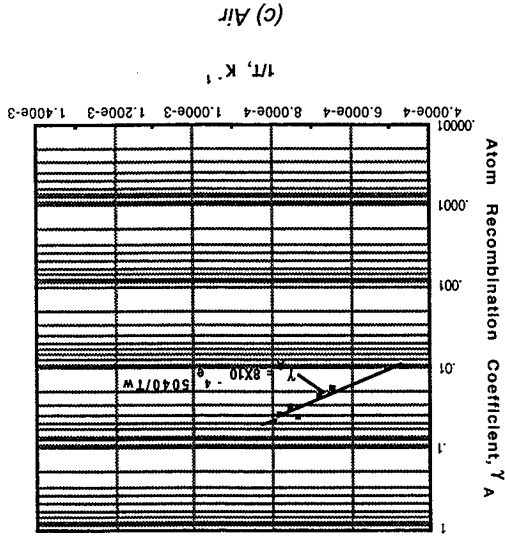
(b) Oxygen



(c) Air

Figure 17. Atom recombination coefficients for LVP.

Figure 18. Atom recombination coefficients for Russian ACC.



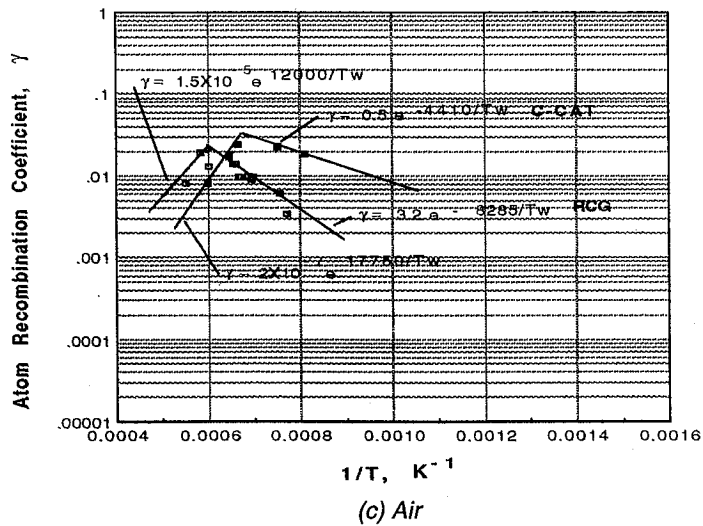
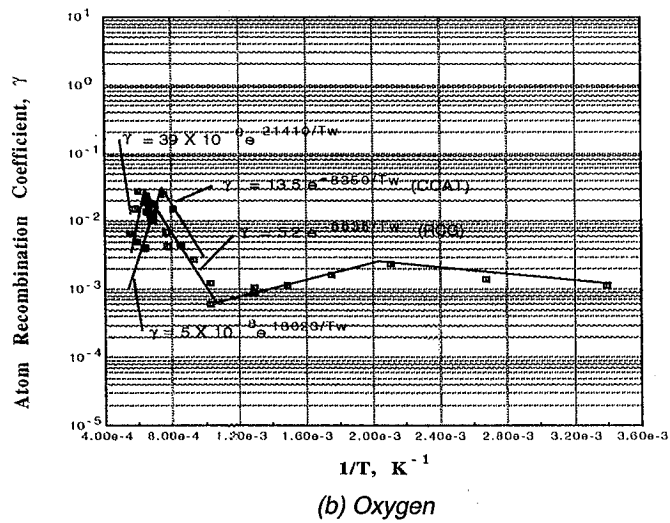
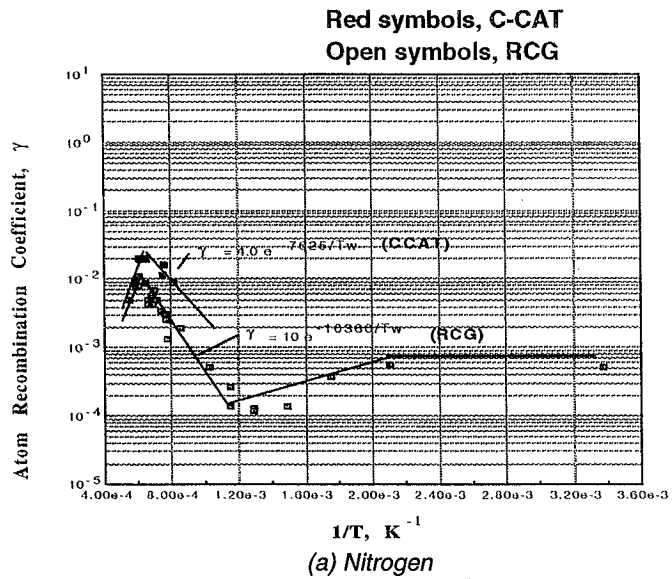


Figure 19. Comparison of atom recombination coefficients for C-CAT and RCG surfaces.

REPORT DOCUMENTATION PAGE

Form Approved
OMB No. 0704-0188

Public reporting burden for this collection of information is estimated to average 1 hour per response, including the time for reviewing instructions, searching existing data sources, gathering and maintaining the data needed, and completing and reviewing the collection of information. Send comments regarding this burden estimate or any other aspect of this collection of information, including suggestions for reducing this burden, to Washington Headquarters Services, Directorate for Information Operations and Reports, 1215 Jefferson Davis Highway, Suite 1204, Arlington, VA 22202-4302, and to the Office of Management and Budget, Paperwork Reduction Project (0704-0188), Washington, DC 20503.

1. AGENCY USE ONLY (Leave blank)	2. REPORT DATE February 1996	3. REPORT TYPE AND DATES COVERED Technical Memorandum	
4. TITLE AND SUBTITLE Surface Catalytic Efficiency of Advanced Carbon Carbon Candidate Thermal Protection Materials for SSTO Vehicles		5. FUNDING NUMBERS 242-20-01	
6. AUTHOR(S) David A. Stewart		8. PERFORMING ORGANIZATION REPORT NUMBER A-961133	
7. PERFORMING ORGANIZATION NAME(S) AND ADDRESS(ES) Ames Research Center Moffett Field, CA 94035-1000		10. SPONSORING/MONITORING AGENCY REPORT NUMBER NASA TM-110383	
9. SPONSORING/MONITORING AGENCY NAME(S) AND ADDRESS(ES) National Aeronautics and Space Administration Washington, DC 20546-0001		11. SUPPLEMENTARY NOTES Point of Contact: David A. Stewart, Ames Research Center, MS 234-1, Moffett Field, CA 94035-1000 (415) 604-6614	
12a. DISTRIBUTION/AVAILABILITY STATEMENT Unclassified — Unlimited Subject Category 23		12b. DISTRIBUTION CODE	
13. ABSTRACT (Maximum 200 words) The catalytic efficiency (atom recombination coefficients) for advanced ceramic thermal protection systems was calculated using arc-jet data. Coefficients for both oxygen and nitrogen atom recombination on the surfaces of these systems were obtained to temperatures of 1650 K. Optical and chemical stability of the candidate systems to the high energy hypersonic flow was also demonstrated during these tests.			
14. SUBJECT TERMS Catalytic efficiency, Surface characterization, Thermal protection		15. NUMBER OF PAGES 24	
		16. PRICE CODE A03	
17. SECURITY CLASSIFICATION OF REPORT Unclassified	18. SECURITY CLASSIFICATION OF THIS PAGE Unclassified	19. SECURITY CLASSIFICATION OF ABSTRACT	20. LIMITATION OF ABSTRACT

